

# AMPOSE: ALTERNATIVELY MIXED GLOBAL-LOCAL ATTENTION MODEL FOR 3D HUMAN POSE ESTIMATION

Hongxin Lin, Yunwei Chiu and Peiyuan Wu

National Taiwan University

## ABSTRACT

The graph convolutional network has been applied to 3D human pose estimation. In addition, the pure transformer model recently show the promising result in the video-based method. However, the single-frame method still need to model the physically connected relations among joints because the feature representation transformed only by the global attention has the lack of the relationships of human skeleton. We propose a novel architecture to combine the physically connected and global relations among joints in human.

We evaluate our method on Human3.6m and compare with the state-of-the-art models. Our model show superior result over all other models. Our model has better generalization ability by cross-dataset comparison on MPI-INF-3DHP.

**Index Terms**— GCNs, Transformer, 3D human pose estimation, 2D-3D lifting

## 1. INTRODUCTION

Monocular 3D human pose estimation from the input image or video is an active research topic in computer vision, with application in virtual reality, augmented reality, action recognition, human-robot interaction, medical assistance, and self-driving. With progress in 2D human joint detector based on neural network models along with enormous availability of public human pose datasets, there has been notable advance in 3D human pose estimation from monocular images. Most works are based on the 2D-to-3D lifting pipeline which inferences the 2D keypoints on the image plane by off-the-shelf 2D pose detector firstly [1, 2, 3, 4], and then lift them to 3D keypoints. Splitting up this problem to two stages reduces the difficulty of tasks (which speeds up computation and use less memory capacity) and increase the the generalization ability, which localizes 2D human joints in images in first stage to filter out the background noise of images. Estimating 3D poses from 2D keypoints remain challenging. It is a well-known ill-posed problem due to the depth ambiguity and occlusion. Multiple 3D positions may be projected to the same 2D position in the image space, so it is still difficult to estimate accurate 3D posture directly from monocular images without multi-view information and camera parameters. Many exist-

ing works focus on temporal 3D pose estimation in the video [3, 5, 6, 7]. The temporal modeling can sufficiently leverage long-sequence information contained in the input video to generate smoother motion, which can partially solve the depth ambiguity and self-occlusion to improve the prediction accuracy. In spite of that, the number of parameters of temporal models have drastically grown as the development of deep learning in 3D human pose estimation because of pursuing the higher prediction accuracy on public datasets. Temporal modelling usually regards temporal information as independent dimension of data or tokens, which demands high memory capacity and performance computing to run these models [6, 7]. Considering computational cost, single-frame models can be more easy to apply to real-world scenario.

Early works have shown that the 2D joint positions in image space is critical to learn feature representations for 3D positions [3, 8], but fully connected and convolution neural networks can not exploit the spatial information among human joints. To solve the lack of of capturing the spatial relationships among joints, graph convolutional networks (GCNs) have recently been applied to the 2D-3D lifting human pose estimation [4, 9, 10, 11, 12, 13, 14]. A drawback of the vanilla GCNs derived from spectrum convolution is weight sharing convolution among joints where each nodes in the graph are transformed by a same feature transformation and then aggregate the feature of neighboring node to transfer the information of the joints to the next layer. There are two plausible reasons to explain why weight sharing method may not work well to capture the characteristics of human anatomy. On the one hand, the dependent relations among joints may be different. For example, the movement of a wrist is dominated by a elbow. While the movement of the elbow happen, the wrist will move according to this movement as well. The other joints have the similar relation such as knees and ankles. On the other hand, the flexibility and speed of human motion can vary with joints. The joints of limbs have flexible movements and the joints of body have relatively stable motion. Therefore, The limited and shared weight in graph convolution can not well learn the diverse and complex relationships among joints in articulated human system. To address the problems, weight unsharing strategy can be applied. This strategy is that different nodes is transformed by different feature transformations according to the relations of neighboring joints rather

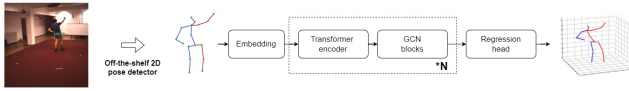


**Fig. 1.** Overview of our proposed network architecture for 3D pose estimation from single-frame

than a same feature transformation before aggregating the features of neighboring joints.

Non-local or global dependency among joints in 3D human pose estimation remain unclear. Some works leverage GCNs to model the non-local relationships where the graph of human skeleton contain symmetrical connections between left and right limbs, and others extend receptive field of GCNs to higher order neighbor nodes via Chebnet [15]. The recent popular Transformer model has been applied to many areas in computer vision and achieve tremendous success such as video-based model and classification model. The Transformer can be utilized to capture the global information in images. The self-attention mechanism of the transformer is designed to relate different positions of a single sequence. In the case of 3D human pose estimation, the self-attention mechanism allows the joint positions to interact with each other. The self-attention is suitable to model the relations since the non-local or global dependence can alter for different poses. However, Pure transformer model weaken the relationships in the human skeleton.

To fully exploit the local and non-local relations among joints of human skeleton, we proposed a novel structure which can alternatively mix the information of local and global dependency by two independent module respectively correspond to GCN blocks and Transformer encoder. GCN blocks consist of graph convolution which only aggregate the transformed feature of nearest nodes defined on the naturally human skeleton, which make this block keep the graph structure information among joints in our network.

In sum, our contributions are three-fold.

- We propose a novel structure to independently capture global and local information in human skeleton.
- We explore that different design for the graph convolution blocks, which improve the performance of graph convolution and fully exploit the physically-connected feature.
- Our model outperforms state-of-the-art model in challenging dataset human3.6m and test its generalization ability across different datasets by more challenging datasets MPI-INF-3DHP. The result show that our model achieves better generalization ability over all the other methods.

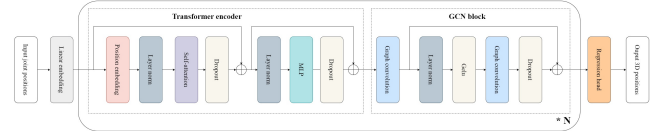


**Fig. 2.** An instantiation of our proposed model for 3D pose estimation

## 2. RELATED WORKS

### 2.1. 3D human pose estimation

With the development of monocular 3D human pose estimation, different architecture has been proposed to reconstruct the human skeleton. There are two categories for single-view 3D human pose estimation method, which include direct estimation and two-stages pose estimation.

The direct estimation is to train convolutional neural networks to directly regress 3D human poses from the input image or video in an end-to-end learning paradigm, which simultaneously adjusts the whole weight of the neural network and alleviates the requirement for intermediate interpretability. For the purpose of data efficiency, Park *et al.* [16] combine 2D position of joints with relative positions of joints to improve the estimation accuracy. Pavlakos *et al.* [17] propose a fine discretization of the 3D space around the subject and model the 3D space upon convolutional neural networks to predict per voxel likelihoods for each joint. Zhou *et al.* [18] leverage in-the-wild images with relative depth information of joints to improve the the generalization ability and obtain the joint positions from the volumetric heatmaps by the integral operation. Sun *et al.* [19] introduce a simple integral operation to unify heat map and joint regression.

The two-stages pose estimation is popular in recent year due to the private preserving, less computation, and excellent generalization ability. Our approach falls into this category. The various 2D pose detectors in first stage can be applied according to the different target of tasks [20, 21, 22]. In second stage, some methods adopt GCNs to model the relationships in the human skeleton [4, 10, 23]. These works aim to explore the optimal strategy of weight unshareing for 3D human pose estimation. Zou *et al.* [11] build their model on vanilla and weight unsharing GCNs. They introduce weight modulation to vanilla GCNs to adjust the feature transformations of different nodes. Xu *et al.* [9] proposed an architecture consisting a repeated encoder-decoder in which graph-structured data are processed across different scales of human skeleton.

## 3. METHODOLOGY

### 3.1. Overview

The overall framework of our proposed method is illustrated in Fig. 1. We aim to predict the 3D joint position. Our method

takes 2D joint positions estimated by off-the-shelf 2D pose detector as input. Each joint pose is embeded a higher dimension feature by a trainable linear projection layer, and then we alternatively stack the Transformer encoder and the GCN block to transform the embedding feature. We regress the output of feature from last the GCN block to predict the 3D pose with layer normalization and linear projection layer.

### 3.2. Transformer encoder

**Scaled Dot-Product Attention** is an attention mechanism that maps a query matrix  $Q$ , key matrix  $K$  and value matrix  $V$  to an output attention matrix.  $Q, K, V \in R^{N_j \times N_d}$ , where  $N_j$  is the number of joints and  $N_d$  is the dimension. A scaling factor of  $\sqrt{d}$  is utilized within this attention operation for normalization, preventing the extremely big value of multiplication of the query and the key. Thus the output of the self-attention can be expressed as:

$$\text{Attention}(Q, K, V) = \text{Softmax}\left(\frac{QK^T}{\sqrt{d}}\right)V \quad (1)$$

The  $Q$ ,  $K$  and  $V$  are computed from the embedded feature  $Z \in R^{N_j \times N_d}$  by learnable feature transformation  $W^Q$ ,  $W^K$ ,  $W^V \in R^{N_d \times N_d}$ .

$$Q = ZW^Q, K = ZW^K, V = ZW^V \quad (2)$$

**Multi-head Self Attention Layer (MSA)** utilizes multiple heads to model the information jointly from different representation subspaces at different positions. The single attention mechanism is applies to each head in parallel. The MSA output will be the concatenation of  $N_h$  attention head outputs.

$$\text{MSA}(Q, K, V) = \text{concat}(\text{head}_1, \dots, \text{head}_{N_h}) \quad (3)$$

where  $\text{head}_i = \text{Attention}(Q_i, K_i, V_i)$ ,  $i \in [1, \dots, N_h]$

**Multi-layer perceptron (MLP)** consists of two fully connected layers (FC) with Gelu activation function [24]. The process is defined as

$$\text{MLP}(z) = \text{FC}_2(\sigma_{\text{Gelu}}(\text{FC}_1(z))) \quad (4)$$

The overall process can be formulated as follows:

$$Z' = Z_0 + W_{pos} \quad (5)$$

$$Z'' = \text{MSA}(\text{LN}(Z')) + Z' \quad (6)$$

$$Z_1 = \text{MLP}(\text{LN}(Z'')) + Z'' \quad (7)$$

where  $Z_0$  denotes the feature from the last layer,  $\text{LN}(\cdot)$  represents layer normalization operator,  $W_{pos}$  is the positional embedding, and  $Z_1$  denotes the output of the encoder.

### 3.3. GCN blocks

In this blocks, a spectral-based GCN [25, 26, 27, 15, 28] is adopted since it can incorporate the information structure

data with a handcrafted graph. The spectral convolutions on graphs can be regarded as the multiplication of a feature with a filter via graph Fourier transformation:

$$g_\theta * x = U g_\theta U^T x \quad (8)$$

where  $x$  is the signal,  $g_\theta$  denotes the filter which equals to  $\text{diag}(\theta)$ , graph Fourier basis  $U$  represents the matrix of the eigenvectors of the normalized graph Laplacian  $L$ , and  $U^T x$  is the graph Fourier transform of  $x$ .

The formulation is not easy to apply due to complex computation and high order polynomial. Kipf *et al.* [28] simplify the spectral graph convolution with the first-order approximation, which also shorten the receptive field of the filter to 1-hop range. The formula is the vanilla GCN as the follows:

$$Z = D^{-0.5} A D^{-0.5} X \Theta \quad (9)$$

Where  $A \in \{0, 1\}^{N_j \times N_j}$  denote the adjacent matrix which includes the self-loop edges for all nodes, the diagonal matrix  $D \in R^{N_j \times N_j}$  is the degree of nodes which is computed as  $\sum_j A^{ij}$ ,  $X \in R^{N_j \times N_d}$  is the signal,  $\Theta \in R^{N_d \times N_D}$  is filter parameters,  $Z \in R^{N_j \times N_D}$  is the convolved signal,  $N_j$  is the number of nodes in the graph,  $N_d$  is the input dimension of the signal, and  $N_D$  is the output dimension of the signal.

The vanilla GCNs are applied to the node classification problem in a graph. Fully weight sharing operation can deal well with a dense graph, but the human pose estimation comprehends complex human motion and different flexibility for each joints. The weight sharing method usually shows bad result, so the kernel needs to be redesigned to accommodate GCNs to 3D human pose estimation. Most works [23, 4] proposed to design larger kernel size by semantic relations among joints to solve these problems. In our work, we adopt the similar kernel design method as ST-GCN [4], but we only classify the joint nodes into three groups based on the idea of physical and local relationships in human skeleton:

1. the center node itself
2. neighboring nodes which are closer to the hip node than the center node
3. neighboring nodes which are farther from the hip node than the center node

The formula of graph convolution will be changed due to this modification. The different feature transformations is applied to different nodes according to the three classes, and then the transformed feature will be aggregated:

$$Z = \sum_j D_j^{-0.5} A_j D_j^{-0.5} X \Theta_j \quad (10)$$

where  $j$  denotes the index of different groups, the adjacent matrix  $A \in \{0, 1\}^{N_j \times N_j}$  is decomposed into three sub-matrices  $A_j \in \{0, 1\}^{N_j \times N_j}$  according to the node type, the diagonal matrix  $D_j \in R^{N_j \times N_j}$  is the degree matrix of  $A_j$  with  $\sum_k A_j^{ik}$ , and  $\Theta_j$  is the filter for  $j$ -th type.

### 3.4. Loss function

To predict the 3D position with our alternatively mixed global-local model, We use the mean square errors to minimize the error between the prediction and ground truth positions. The loss function can be computed as:

$$Loss = \frac{1}{N} \sum_i \left\| \mathbf{X}_i - \tilde{\mathbf{X}}_i \right\|^2 \quad (11)$$

where  $N$  is the number of the human joints,  $i$  represents index of joint type,  $X_i$  denotes the 3D ground truth positions, and  $\tilde{X}_i$  denotes the predicted 3D positions.

## 4. EXPERIMENTS

### 4.1. Dataset

We evaluate our approach on two publicly available datasets: Human3.6M [31] and MPI-INF-3DHP [32].

**Human3.6M** is a most widely used dataset for 3D human pose estimation. It consists of 3.6 million images which are collected by 4 synchronized digital cameras in different views. The motion in the dataset were performed by 11 human subjects, but only 7 subject have the annotated 3D positions. The subjects perform a variety of actions such as discussion, sitting, taking photo, and smoking. Following previous work [18, 1], we normalize the 2D positions as the input of our model. The hip joint is used as the root joint of 3D pose, which localizes the 3D human positions. The model is trained on five subjects (S1, S5, S6, S7, S8) and tested on two subjects (S9 and S11).

**MPI-INF-3DHP** is a challenging dataset. It contain indoor and outdoor background along with complex and rare actions. Following prior work [18, 2], we evaluate the generalization ability of our model with this cross-scenario dataset. The model is only trained on Human3.6m and tested on the test set of this dataset, which contains three different scenarios: studio with a green screen (GS), studio without green screen (noGS) and outdoor scene.

### 4.2. Evaluation protocols

We adopt the mean per joint position error (MPJPE) and P-MPJPE as the evaluation protocols. MPJPE is computed as the average Euclidean distance between the predicted 3D joint positions and the 3D ground truth positions in millimeters (mm). We refer to MPJPE as Protocol 1. The estimated 3D pose aligned by a rigid transformation is P-MPJPE, which is referred as protocol 2.

For cross-dataset comparison, we adopt two common metric to evaluate the generalization ability: the Percentage of Correct Keypoints (PCK) and Area Under the Curve (AUC). The estimated positions is considered correct if the distance between the predicted and the true joint is within a certain threshold, which is 150 mm for our setting.

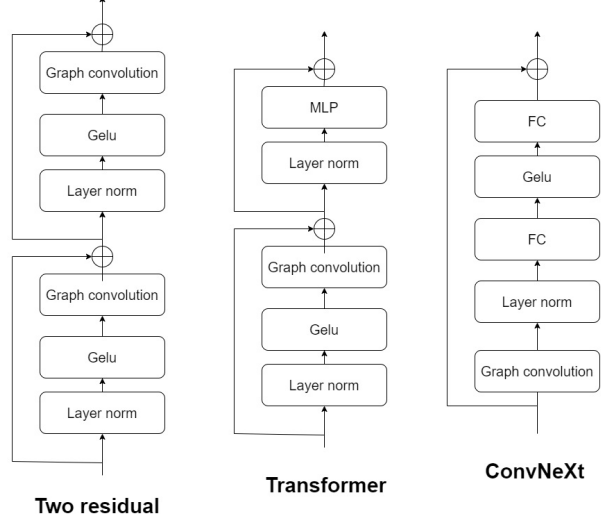


**Table 1.** Quantitative comparisons of Mean Per Joint Position Error (MPJPE) in millimeter on Human3.6m. under Protocol 1 and Protocol 2. Top and middle table: 2D detector CPN with 17 keypoints is used as input. Bottom table: Ground truth 2D (GT) with 17 keypoints is used as input. The best score is marked in **bold**.

Protocol 1 (CPN)	Dire.	Disc.	Eat	Greet	Phone	Photo	Pose	Purch.	Sit	SitD.	Smoke	Wait	WalkD.	Walk	WalkT.	Avg.
Zhao <i>et al.</i> [23]	47.3	60.7	51.4	60.5	61.1	<b>49.9</b>	47.3	68.1	86.2	<b>55.0</b>	67.8	61.0	42.1	60.6	45.3	57.6
Ci <i>et al.</i> [29]	46.8	52.3	<b>44.7</b>	50.4	52.9	68.9	49.6	46.4	60.2	78.9	51.2	50.0	54.8	40.4	43.3	52.7
Cai <i>et al.</i> (refinement) [4]	46.5	48.8	47.6	50.9	52.9	61.3	48.3	45.8	59.2	64.4	51.2	48.4	53.5	39.2	41.2	50.6
Pavllo <i>et al.</i> [3]	47.1	50.6	49.0	51.8	53.6	61.4	49.4	47.4	59.3	67.4	52.4	49.5	55.3	39.5	42.7	51.8
Zou <i>et al.</i> (refinement) [11]	45.4	49.2	45.7	49.4	<b>50.4</b>	58.2	47.9	46.0	57.5	63.0	49.7	46.6	52.2	38.9	40.8	49.4
Lutz <i>et al.</i> [2]	45.0	48.8	46.6	49.4	53.2	60.1	47.0	46.7	59.6	67.1	51.2	47.1	53.8	39.4	42.4	50.5
Ours	44.9	49.3	45.2	48.8	51.3	58.6	47.8	<b>44.8</b>	57.1	66.5	49.9	46.4	52.9	39.0	40.6	49.5
Ours (refinement)	<b>42.8</b>	<b>48.6</b>	45.1	<b>48.0</b>	51.0	56.5	<b>46.2</b>	44.9	<b>56.5</b>	63.9	<b>49.6</b>	<b>46.2</b>	<b>50.5</b>	<b>37.9</b>	<b>39.5</b>	<b>48.5</b>
Protocol 2 (CPN)	Dire.	Disc.	Eat	Greet	Phone	Photo	Pose	Purch.	Sit	SitD.	Smoke	Wait	WalkD.	Walk	WalkT.	Avg.
Pavlakos <i>et al.</i> [17]	<b>34.7</b>	39.8	41.8	<b>38.6</b>	42.5	47.5	38.0	36.6	50.7	56.8	42.6	39.6	43.9	32.1	36.5	41.8
Ci <i>et al.</i> [6]	36.9	41.6	38.0	41.0	41.9	51.1	38.2	37.6	49.1	62.1	43.1	39.9	43.5	32.2	37.0	42.2
Cai <i>et al.</i> (refinement) [4]	36.8	38.7	38.2	41.7	40.7	46.8	37.9	35.6	47.6	51.7	41.3	36.8	42.7	31.0	34.7	40.2
Pavllo <i>et al.</i> [3]	36.0	38.7	38.0	41.7	40.1	45.9	37.1	35.4	46.8	53.4	41.4	36.9	43.1	<b>30.3</b>	34.8	40.0
Zou <i>et al.</i> (refinement) [11]	35.7	38.6	<b>36.3</b>	40.5	<b>39.2</b>	<b>44.5</b>	37.0	35.4	<b>46.4</b>	<b>51.2</b>	40.5	35.6	41.7	30.7	33.9	39.1
Ours	34.9	<b>38.2</b>	36.7	39.7	39.6	44.7	<b>36.0</b>	<b>34.3</b>	46.8	52.9	<b>40.4</b>	<b>35.5</b>	<b>41.6</b>	30.4	<b>33.4</b>	<b>39.0</b>
Protocol 1 (GT)	Dire.	Disc.	Eat	Greet	Phone	Photo	Pose	Purch.	Sit	SitD.	Smoke	Wait	WalkD.	Walk	WalkT.	Avg.
Ci <i>et al.</i> [29]	36.3	38.8	29.7	37.8	34.6	42.5	39.8	32.5	36.2	<b>39.5</b>	34.4	38.4	38.2	31.3	34.2	36.3
Lutz <i>et al.</i> [2]	<b>31.0</b>	36.6	30.2	33.4	<b>33.5</b>	<b>39.0</b>	37.1	31.3	37.1	40.1	33.8	<b>33.5</b>	35.0	28.7	29.1	34.0
Zeng <i>et al.</i> [30]	32.9	<b>34.5</b>	<b>27.6</b>	<b>31.7</b>	<b>33.5</b>	42.5	<b>35.1</b>	<b>29.5</b>	38.9	45.9	33.3	34.9	<b>34.4</b>	<b>26.5</b>	<b>27.1</b>	33.9
Ours	31.2	35.9	29.2	33.4	33.6	39.2	37.8	30.8	<b>35.9</b>	41.6	<b>32.9</b>	34.3	34.5	27.8	29.3	<b>33.8</b>

**Table 2.** Quantitative comparisons of MPJPE in millimeter on Human3.6m. Top table: 2D detector CPN with 16 keypoints is used as input. Bottom table: Ground truth 2D (GT) with 16 keypoints is used as input. The best score is marked in **bold**.

Protocol 1 (CPN)	Dire.	Disc.	Eat	Greet	Phone	Photo	Pose	Purch.	Sit	SitD.	Smoke	Wait	WalkD.	Walk	WalkT.	Avg.
Liu <i>et al.</i> [10]	46.3	52.2	47.3	50.7	55.5	67.1	49.2	46.0	60.4	71.1	51.5	50.1	54.5	40.3	43.7	52.4
Xu <i>et al.</i> [9]	<b>45.2</b>	49.9	<b>47.5</b>	50.9	54.9	66.1	48.5	46.3	59.7	71.5	51.4	48.6	53.9	39.9	44.1	51.9
Zhao <i>et al.</i> [1]	<b>45.2</b>	50.8	48.0	<b>50.0</b>	54.9	65.0	48.0	47.1	60.2	70.0	51.6	48.7	54.1	<b>39.7</b>	43.1	51.8
Ours	45.8	<b>49.1</b>	47.8	<b>50.0</b>	<b>52.9</b>	<b>59.0</b>	<b>46.9</b>	<b>45.8</b>	<b>58.9</b>	<b>68.0</b>	<b>51.1</b>	<b>47.2</b>	<b>53.6</b>	39.9	<b>41.8</b>	<b>50.5</b>
Protocol 1 (GT)	Dire.	Disc.	Eat	Greet	Phone	Photo	Pose	Purch.	Sit	SitD.	Smoke	Wait	WalkD.	Walk	WalkT.	Avg.
Liu <i>et al.</i> [10]	36.8	40.3	33.0	36.3	37.5	45.0	39.7	34.9	40.3	47.7	37.4	38.5	38.6	29.6	32.0	37.8
Xu <i>et al.</i> [9]	35.8	38.1	31.0	35.3	35.8	43.2	37.3	31.7	38.4	45.5	35.4	36.7	36.8	27.9	30.7	35.8
Zhao <i>et al.</i> [1]	32.0	38.0	30.4	34.4	34.7	43.3	<b>35.2</b>	<b>31.4</b>	38.0	46.2	34.2	35.7	36.1	<b>27.4</b>	30.6	35.2
Ours	<b>31.3</b>	<b>36.7</b>	<b>30.0</b>	<b>34.3</b>	<b>34.0</b>	<b>37.8</b>	38.2	32.0	<b>36.0</b>	<b>40.7</b>	<b>34.1</b>	<b>34.4</b>	<b>34.6</b>	28.2	<b>29.8</b>	<b>34.1</b>

**Table 3.** Cross-dataset comparison on MPI-INF-3DHP.

Method	GS	noGS	Outdoor	All PCK	All AUC
Martinez <i>et al.</i> [8]	49.8	42.5	31.2	42.5	17.0
Mehta <i>et al.</i> [32]	70.8	62.3	58.5	64.7	31.7
Ci <i>et al.</i> [29]	74.8	70.8	77.3	74.0	36.7
Zhao <i>et al.</i> [1]	80.1	77.9	74.1	79.0	43.8
Liu <i>et al.</i> [10]	77.6	80.5	80.1	79.3	47.6
Xu <i>et al.</i> [9]	81.5	81.7	75.2	80.1	45.8
Zeng <i>et al.</i> [2]	-	-	84.6	82.1	46.2
Zou <i>et al.</i> [11]	86.4	86.0	85.7	86.1	53.7
Ours	86.0	87.6	87.3	87.0	54.7

on Human3.6m with 17 keypoints. The results are shown in Table 3. We separately report the result with different background, including GS, noGS, outdoor. Our model reaches 87

**Table 4.** The results of the different design for GCN blocks

Method	MPJPE
Two residual	50.1
Transformer	50.1
ConvNeXt	50.0
Ours	49.5

percent correct rate without fine-tuning on MPI-INF-3DHP.

#### 4.5. Ablation Study

We explore the optimal design of GCN block for the proposed architecture. As depicted in Fig. 3, we test the different design of GCN blocks which are derived from the success and

verified blocks, including Transformer [33], ResNet [34], ConvNeXt [35]. The result is shown in Table 4. Our design show in Fig. 2. We found that a plain graph convolution followed by a graph convolution with the residual have the best result in our experiment.

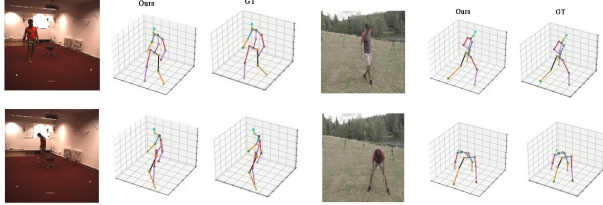


**Fig. 4.** Visualization results on Human3.6M and MPI-INF-3DHP

#### 4.6. Qualitative Results

Fig. 4 shows some visualization results estimated by our model on Human3.6M and MPI-INF-3DHP. It can predict 3D poses in the various background. The model generate the similar human action with ground truth and even the actor performing the rare actions in outdoor can be estimated by our model.

### 5. CONCLUSION

In this paper, we have present a novel architecture for single-frame 3D pose estimation which can effectively leverage both local and non-local information. We show quantitative result to compare with the state-of-the-art models. For realistic application, the light weight model based on our proposed architecture may be a future work.

### 6. REFERENCES

- [1] Weixi Zhao, Yunjie Tian, Qixiang Ye, Jianbin Jiao, and Weiqiang Wang, “Graformer: Graph convolution transformer for 3d pose estimation,” *arXiv preprint arXiv:2109.08364*, 2021.
- [2] Sebastian Lutz, Richard Blythman, Koustav Ghosal, Matthew Moynihan, Ciaran Simms, and Aljosa Smolic, “Jointformer: Single-frame lifting transformer with error prediction and refinement for 3d human pose estimation,” *arXiv preprint arXiv:2208.03704*, 2022.
- [3] Dario Pavllo, Christoph Feichtenhofer, David Grangier, and Michael Auli, “3d human pose estimation in video with temporal convolutions and semi-supervised training,” in *Proceedings of the IEEE/CVF Conference on Computer Vision and Pattern Recognition*, 2019, pp. 7753–7762.
- [4] Yujun Cai, Liuao Ge, Jun Liu, Jianfei Cai, Tat-Jen Cham, Junsong Yuan, and Nadia Magnenat Thalmann, “Exploiting spatial-temporal relationships for 3d pose estimation via graph convolutional networks,” in *2019 IEEE/CVF International Conference on Computer Vision (ICCV)*, 2019.
- [5] Ce Zheng, Sijie Zhu, Matias Mendieta, Taojiannan Yang, Chen Chen, and Zhengming Ding, “3d human pose estimation with spatial and temporal transformers,” in *Proceedings of the IEEE/CVF International Conference on Computer Vision*, 2021, pp. 11656–11665.
- [6] Wenhao Li, Hong Liu, Hao Tang, Pichao Wang, and Luc Van Gool, “Mhformer: Multi-hypothesis transformer for 3d human pose estimation,” in *Proceedings of the IEEE/CVF Conference on Computer Vision and Pattern Recognition*, 2022, pp. 13147–13156.
- [7] Jinlu Zhang, Zhigang Tu, Jianyu Yang, Yujin Chen, and Junsong Yuan, “Mixste: Seq2seq mixed spatio-temporal encoder for 3d human pose estimation in video,” in *Proceedings of the IEEE/CVF Conference on Computer Vision and Pattern Recognition*, 2022, pp. 13232–13242.
- [8] Julieta Martinez, Rayat Hossain, Javier Romero, and James J Little, “A simple yet effective baseline for 3d human pose estimation,” in *Proceedings of the IEEE international conference on computer vision*, 2017, pp. 2640–2649.
- [9] Tianhan Xu and Wataru Takano, “Graph stacked hourglass networks for 3d human pose estimation,” in *Proceedings of the IEEE/CVF conference on computer vision and pattern recognition*, 2021, pp. 16105–16114.
- [10] Kenkun Liu, Rongqi Ding, Zhiming Zou, Le Wang, and Wei Tang, “A comprehensive study of weight sharing in graph networks for 3d human pose estimation,” in *Computer Vision – ECCV 2020*, Andrea Vedaldi, Horst Bischof, Thomas Brox, and Jan-Michael Frahm, Eds., 2020.
- [11] Zhiming Zou and Wei Tang, “Modulated graph convolutional network for 3d human pose estimation,” in *2021 IEEE/CVF International Conference on Computer Vision (ICCV)*, 2021, pp. 11457–11467.
- [12] Wenbo Hu, Changgong Zhang, Fangneng Zhan, Lei Zhang, and Tien-Tsin Wong, “Conditional directed graph convolution for 3d human pose estimation,” in *Proceedings of the 29th ACM International Conference on Multimedia*, 2021, pp. 602–611.
- [13] Jingbo Wang, Sijie Yan, Yuanjun Xiong, and Dahua Lin, “Motion guided 3d pose estimation from videos,” in *European Conference on Computer Vision*. Springer, 2020, pp. 764–780.

[14] Junfa Liu, Juan Rojas, Yihui Li, Zhijun Liang, Yisheng Guan, Ning Xi, and Haifei Zhu, “A graph attention spatio-temporal convolutional network for 3d human pose estimation in video,” in *2021 IEEE International Conference on Robotics and Automation (ICRA)*. IEEE, 2021, pp. 3374–3380.

[15] Michaël Defferrard, Xavier Bresson, and Pierre Vandergheynst, “Convolutional neural networks on graphs with fast localized spectral filtering,” *Advances in neural information processing systems*, vol. 29, 2016.

[16] Sungheon Park, Jihye Hwang, and Nojun Kwak, “3d human pose estimation using convolutional neural networks with 2d pose information,” in *ECCV Workshops*, 2016.

[17] Georgios Pavlakos, Xiaowei Zhou, Konstantinos G Derpanis, and Kostas Daniilidis, “Coarse-to-fine volumetric prediction for single-image 3d human pose,” in *Proceedings of the IEEE conference on computer vision and pattern recognition*, 2017, pp. 7025–7034.

[18] Kun Zhou, Xiaoguang Han, Nianjuan Jiang, Kui Jia, and Jiangbo Lu, “Hemlets pose: Learning part-centric heatmap triplets for accurate 3d human pose estimation,” in *Proceedings of the IEEE/CVF international conference on computer vision*, 2019, pp. 2344–2353.

[19] Xiao Sun, Bin Xiao, Fangyin Wei, Shuang Liang, and Yichen Wei, “Integral human pose regression,” in *Proceedings of the European conference on computer vision (ECCV)*, 2018, pp. 529–545.

[20] Yilun Chen, Zhicheng Wang, Yuxiang Peng, Zhiqiang Zhang, Gang Yu, and Jian Sun, “Cascaded pyramid network for multi-person pose estimation,” in *Proceedings of the IEEE conference on computer vision and pattern recognition*, 2018, pp. 7103–7112.

[21] Hao-Shu Fang, Shuqin Xie, Yu-Wing Tai, and Cewu Lu, “Rmpe: Regional multi-person pose estimation,” in *Proceedings of the IEEE international conference on computer vision*, 2017, pp. 2334–2343.

[22] Jingdong Wang, Ke Sun, Tianheng Cheng, Borui Jiang, Chaorui Deng, Yang Zhao, Dong Liu, Yadong Mu, Mingkui Tan, Xinggang Wang, et al., “Deep high-resolution representation learning for visual recognition,” *IEEE transactions on pattern analysis and machine intelligence*, 2020.

[23] Long Zhao, Xi Peng, Yu Tian, Mubbashir Kapadia, and Dimitris N Metaxas, “Semantic graph convolutional networks for 3d human pose regression,” in *Proceedings of the IEEE/CVF conference on computer vision and pattern recognition*, 2019, pp. 3425–3435.

[24] Dan Hendrycks and Kevin Gimpel, “Gaussian error linear units (gelus),” *arXiv preprint arXiv:1606.08415*, 2016.

[25] Ruoyu Li, Sheng Wang, Feiyun Zhu, and Junzhou Huang, “Adaptive graph convolutional neural networks,” in *Proceedings of the AAAI conference on artificial intelligence*, 2018.

[26] David I Shuman, Sunil K. Narang, Pascal Frossard, Antonio Ortega, and Pierre Vandergheynst, “The emerging field of signal processing on graphs: Extending high-dimensional data analysis to networks and other irregular domains,” *IEEE Signal Processing Magazine*, 2013.

[27] Ron Levie, Federico Monti, Xavier Bresson, and Michael M Bronstein, “Caylenets: Graph convolutional neural networks with complex rational spectral filters,” *IEEE Transactions on Signal Processing*, 2018.

[28] Thomas N Kipf and Max Welling, “Semi-supervised classification with graph convolutional networks,” *arXiv preprint arXiv:1609.02907*, 2016.

[29] Hai Ci, Chunyu Wang, Xiaoxuan Ma, and Yizhou Wang, “Optimizing network structure for 3d human pose estimation,” in *2019 IEEE/CVF International Conference on Computer Vision (ICCV)*, 2019, pp. 2262–2271.

[30] Ailing Zeng, Xiao Sun, Fuyang Huang, Minhao Liu, Qiang Xu, and Stephen Lin, “Srnet: Improving generalization in 3d human pose estimation with a split-and-recombine approach,” in *European Conference on Computer Vision*. Springer, 2020, pp. 507–523.

[31] Catalin Ionescu, Dragos Papava, Vlad Olaru, and Cristian Sminchisescu, “Human3. 6m: Large scale datasets and predictive methods for 3d human sensing in natural environments,” *IEEE transactions on pattern analysis and machine intelligence*, vol. 36, no. 7, pp. 1325–1339, 2013.

[32] Dushyant Mehta, Helge Rhodin, Dan Casas, Pascal Fua, Oleksandr Sotnychenko, Weipeng Xu, and Christian Theobalt, “Monocular 3d human pose estimation in the wild using improved cnn supervision,” in *2017 international conference on 3D vision (3DV)*. IEEE, 2017, pp. 506–516.

[33] Ashish Vaswani, Noam Shazeer, Niki Parmar, Jakob Uszkoreit, Llion Jones, Aidan N Gomez, Łukasz Kaiser, and Illia Polosukhin, “Attention is all you need,” *Advances in neural information processing systems*, vol. 30, 2017.

[34] Kaiming He, Xiangyu Zhang, Shaoqing Ren, and Jian Sun, “Deep residual learning for image recognition,” in *Proceedings of the IEEE conference on computer vision and pattern recognition*, 2016, pp. 770–778.

[35] Zhuang Liu, Hanzi Mao, Chao-Yuan Wu, Christoph Feichtenhofer, Trevor Darrell, and Saining Xie, “A convnet for the 2020s,” in *Proceedings of the IEEE/CVF Conference on Computer Vision and Pattern Recognition*, 2022, pp. 11976–11986.